Nanoscale insights into the creation of chiral surfaces

R. Raval*

Surface Science Research Centre and Department of Chemistry, University of Liverpool, Oxford Street, Liverpool L69 3BX, UK

ARTICLE INFO

ABSTRACT

Chirality and enantioselectivity are often conferred on a reactive metal by adsorption of organic molecules. How this chirality is nucleated, expressed and propagated at a surface remains a real challenge in the field of heterogeneous enantioselective catalysis. Over the past decade, nanoscopic insights have been built up from advanced surface science experiments and high-level density functional theory. This body of work is beginning to reveal the mechanisms of asymmetric induction and the critical roles of both the organic molecule and the underlying surface in creating overall chirality at an interface. The work presented here summarises the salient points of tartaric acid behaviour on Cu(1 1 0) and Ni(1 1 0) surfaces.

© 2008 Elsevier B.V. All rights reserved.

1. Introduction

Of the several different methods for creating heterogeneous chiral catalysts [1–5], the adsorption of chiral molecules at achiral solid surfaces to induce asymmetry remains a popular choice. Although this appears a deceptively simple approach to creating asymmetry in a reaction, the reality of creating a working catalyst remains notoriously difficult and unpredictable. In 1996, we began a programme of fundamental surface science studies at the Leverhulme Centre for Innovative Catalysis at Liverpool, aimed at establishing a molecular and atomic-level understanding on how chirality is nucleated, expressed and propagated at defined single crystal metal surfaces. We were directed in our choice of chiral molecules by the extensive Japanese work of Izumi, Tai and Harada [6,7] on the hydrogenation of β-ketoesters over supported Ni catalysts [6–10], which showed that the reaction can become enantioselective upon adsorption of chiral organic molecules such as the dicarboxylic acid, tartaric acid, and the α-amino-acid, alanine, as surface modifiers. Using these modifiers, researchers were able to demonstrate the stereospecific hydrogenation of methyl acetoacetate to give (R) or (S)-methyl-3-hydroxybutyrate [6,7], as well

as the interesting fact that the enantiomeric form of the product is determined by the chirality of the organic modifier, with the (R,R)-tartaric acid ((S)-alanine) favouring the (R)-product in <90% enantiomeric excess, while (S,S)-tartaric acid ((R)-alanine) favours the (S)-product [6,7].

Thus, the adsorption of (R,R)-tartaric acid on a Cu(1 1 0) surface formed the basis of our initial studies and the main aspects of this system are summarised here, showing the explicit role played by the adsorbate, the surface and the adsorption process in introducing both complexity and asymmetry at an interface.

2. Modifiers possess complex, dynamic adsorption behaviour

One of the most intriguing aspects of the literature on the enantioselective hydrogenation of β-ketoesters over supported Ni catalysts is the critical dependence between enantiomeric excesses obtained and system variables such as temperature, concentration of modifier, time of modification, pH, etc. The underlying basis of this behaviour became evident when we discovered that the adsorption behaviour of enantiopure (R,R)-tartaric acid on Cu(1 1 0) [11–13] occupies a complex and dynamic phase space and leads to a highly sensitive system where the description of the adsorbed molecules changes rapidly between the monotartrate, bitartrate or dimer forms as coverage and temperature are varied, Fig. 1a.

* Tel.: +44 1517946981.
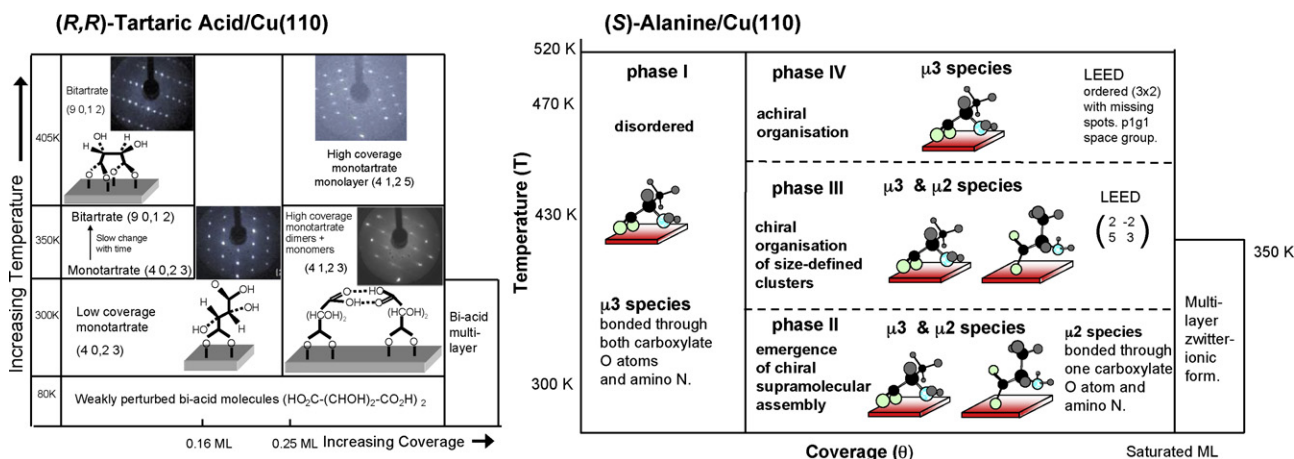E-mail address: Raval@liv.ac.uk.

Fig. 1. Adsorption phase diagrams with the corresponding adsorbate species and LEED patterns for the main phases observed for (a) (R,R)-tartaric acid on Cu(1 1 0), reproduced with permission from Ref. [11], copyright 1999, American Chemical Society; (b) (S)-alanine on Cu(1 1 0), reproduced with permission from Ref. [14], copyright 2005, Elsevier.

This behaviour is not confined to tartaric acid; for example, it is also echoed by the modifier, (S)-alanine, on Cu(1 1 0) [14], Fig. 1b. This plural, dynamical behaviour of modifier behaviour at a surface immediately rationalises the delicate balances reported in the catalytic literature.

3. Modifiers can self-organise at surfaces

A rather unexpected property of organic modifier behaviour at metal surfaces also revealed itself in our studies, namely the ability to self-organise on the surface leading to nanostructures that possess different crystalline architectures and provide different chiral environments [11–17]. Examples of STM images captured for a range of modifier phases are shown in Fig. 2a–d, alongside molecular models of the real-space structures. The richness and complexity of modifier behaviour at surfaces is self-evident.

4. The hierarchical expression of chirality

The adsorption of organic molecules at achiral surfaces can lead to a hierarchical expression of chirality [15,16] advancing from point (0D) chirality, arising because the adsorption of the molecule locally destroys all mirror planes, to the creation of longer-range (1D–2D) chiral superstructures, which are bereft of mirror symmetry. These longer-range chiral superstructures can vary in lengthscale from nanoscale to macroscale [15,17]. This step-by-step construction of chirality at an interface is illustrated by the low coverage/high temperature phase of the (R,R)-tartaric acid/Cu(1 1 0) system, thought to be the most catalytically pertinent since it is the only one able to accommodate reactant molecules such methylacetoacetate within its structure. This phase consists solely of the doubly dehydrogenated bitartrate species, is highly organised with a $(9\,0, 1\,2)$ repeat unit cell and is only observed for coverages $\leq 1/6$ of a monolayer [11,12]. The various hierarchies of chiral expression exhibited
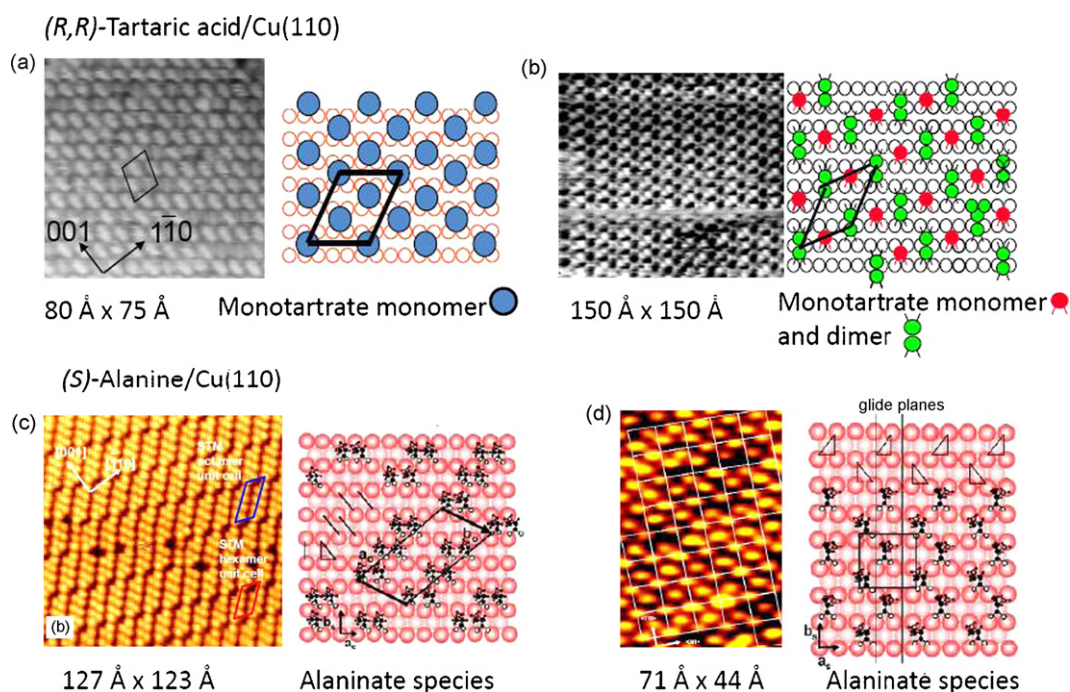

Fig. 2. STM images and associated real-space models for differently organised molecular adlayers showing (a) the $(4\,0, 2\,3)$ adlayer of (R,R)-tartaric acid/Cu(1 1 0); (b) the $(4\,1, 2\,3)$ adlayer of (R,R)-tartaric acid/Cu(1 1 0); (c) the $(2\,-2, 5\,3)$ adlayer of (S)-Alanine/Cu(1 1 0); (d) the (3×2) adlayer of (S)-alanine/Cu(1 1 0). [(a) and (b) adapted with permission from Ref. [11], copyright 1999, American Chemical Society; (c) adapted with permission from Ref. [14], copyright 2005, Elsevier.].
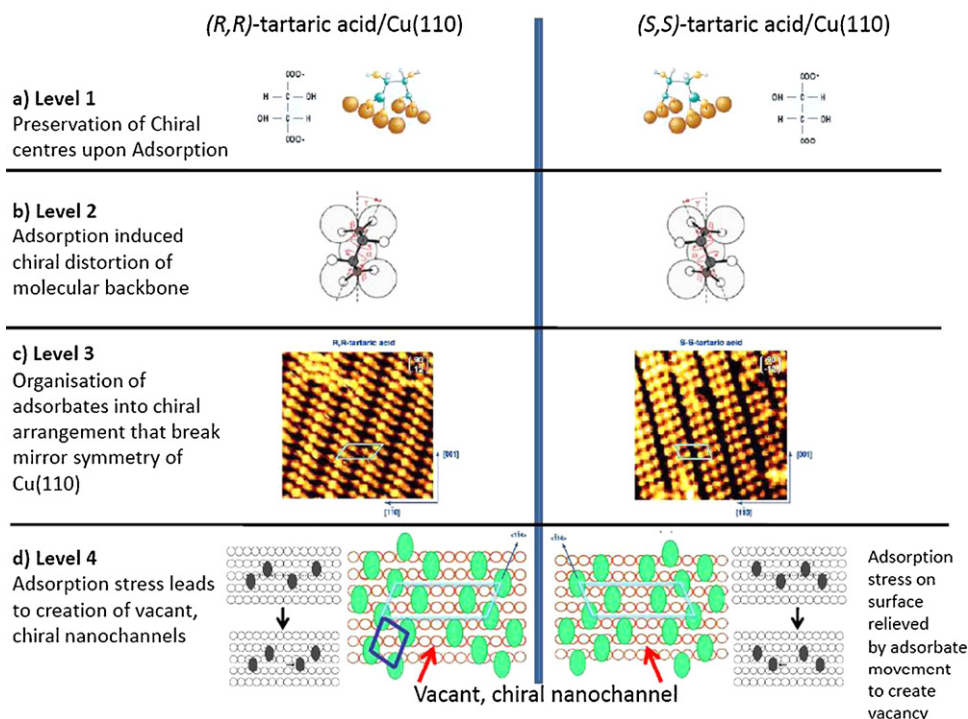
Fig. 3. The hierarchical creation of chirality in the (9 0, 1 2) bitartrate phase of tartaric acid on Cu(1 1 0): (a) schematic of the dehydrogenated bitartrate species on the Cu(1 1 0) surface; (b) molecular distortion upon adsorption for the (R,R) and (S,S) enantiomers, respectively on Cu(1 1 0). Adapted with permission from Ref. [18] copyright 2001, American Chemical Society and Ref. [19], copyright 2004, Wiley; (c) STM images showing the handed organisation of the (R,R) and (S,S) enantiomers on Cu(1 1 0). Reproduced with permission from Ref. [12], copyright 2000, Nature Publishing Group; (d) how adsorption-induced surface stress can be relieved by a molecule being displaced to create a vacant channel. Reproduced with permission from Ref. [20], copyright 2004, American Chemical Society.

by this system can be delineated as follows and in Fig. 3:

(i) The chiral centres of the molecule are preserved upon adsorption for all the various chemical forms that are adopted, and no racemisation or inversion occurs upon adsorption—thus, this nucleates the first expression of point chirality, Fig. 3a.

(ii) Surface IR data [11,12], Periodic density functional theory (DFT) calculations by Barbosa and Sautet [18] and X-ray photoelectron diffraction [19] show that the adsorbed bitartrate molecule is bonded to the surface via the two carboxylate groups creating four Cu–O bonds. This adsorption geometry facilitates intramolecular hydrogen-bonding between the OH groups at the chiral centres and the oxygens of the carboxylic group, leading to an asymmetric distortion in the molecule, Fig. 3b, which is enantiomer-specific; the (R,R) enantiomer distorts one way and the (S,S) enantiomer distorts in the mirror configuration. Thus, the adsorption process creates a second level of chiral expression which 'enhances' the chirality already inherent within the molecular structure of (R,R)-tartaric acid.

(iii) The next level of chiral expression arises from the organisation of individual adsorbates at the surface. STM images, Fig. 3c, reveal that rows consisting of three bitartrate molecules are formed on the surface which then proceed to self-assemble into long chains that align along the ⟨1 1 4⟩ direction [12]. Neither the short direction that connects the three molecules in the trimer, nor the long direction adopted by the trimer chains coincide with a mirror symmetry direction of the underlying surface. The chains are propagated across large length-scales and the entire macroscopic surface organisation is, therefore, also chiral and belongs to the C_2 chiral space group and is non-superimposable on its mirror image. Furthermore, there is a transfer of chiral information from the nanoscale adsorbate to the macroscale organisation of the molecules, so that switching molecular chirality also flips the organisational

chirality, Fig. 3c. Thus, STM and LEED data show that when enantiopure (S,S)-tartaric acid is adsorbed on Cu(1 1 0), the mirror organisation is created [12]. This observation provides a starting point for rationalising the catalytic observation that changing the chirality of the surface modifier from (R) to (S) switches the enantioselectivity of the product. This enantiomer-specific organisation arises because there is an energy penalty of 10 kJ mol^{-1} for an enantiomer to occupy the mirror organisations, attributed to steric repulsions that arise between the OH groups of neighbouring adsorbates when they are forced to adopt the mirror structure [18]. This energy difference is sufficient to ensure that 95% of the adsorbed molecules would adopt their preferred handed organisation.

(iv) Finally, there is another and, catalytically more important, manifestation of chirality in the (9 0, 1 2) structure. STM data show the appearance of a vacant nanochannel after every third bitartrate molecule, i.e. each long trimer chain is separated from the adjacent trimer chain by a vacant channel, Fig. 3d. These nanochannels are also directed along the non-symmetric ⟨1 1 4⟩ direction and leads to the creation of inherently chiral spaces on the copper substrate. DFT and Kinetic Monte Carlo calculations reveal the origin of these channels [20]. Upon adsorption of the bitartrate species to the surface, the Cu–Cu distance of the bonding metal atoms is increased from the bulk truncation value of 2.58–2.62 Å, leading to a strong compressive strain along the close-packed [1−10] direction. This stress builds up with each additional carboxylate functionality bonding to a particular row and can only be tolerated for three molecules in a row before a break in the organisation is necessary to relieve it, Fig. 3d. These chiral nanochannels are potentially interesting in terms of enantioselective catalysis, since they provide a confined environment within which reacting molecules can dock in preferential orientations forcing, for example, hydrogenation to occur at
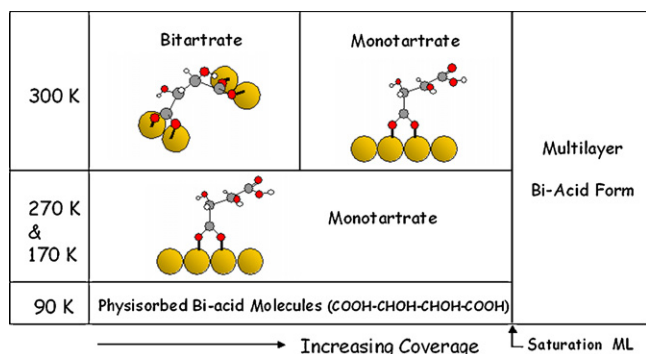
Fig. 4. Phase diagram for the adsorbed nature of Tartaric acid on Ni(1 1 0) as a function of coverage and temperature. Reproduced with permission from Ref. [22], copyright 2004, Elsevier.

one reactant face only. Therefore, in systems such as these, the heterogeneous active site may well be described, not in terms of one modifier, but by groups of modifiers acting cooperatively to confer enantioselectivity to the reactive metal sites.

5. From copper to nickel: transfer of chiral information from modifier to surface at the geometric and electronic level

Nickel is the metal that is most commonly modified by tartaric acid to yield the successful enantioselective catalytic system for the hydrogenation of β-ketoesters [6,7]. Our detailed studies [21,22] of the adsorption of (R,R)-tartaric acid on Ni(1 1 0) as a function of temperature and coverage again shows a complex phase space, Fig. 4, with the local nature of the chiral adsorbate changes dynamically as conditions change, echoing the findings on Cu(1 1 0).

Again, the doubly dehydrogenated bitartrate phase is considered to represent the catalytic active state, because its overall low coverage allows reactant species to approach the surface, and also because the adsorption conditions of low coverage and high temperature match those found to be the most effective [6,7,9] by cat-

alytic studies. Periodic DFT calculations on the bitartrate/Ni(1 1 0) phase [21] confirm that, as on Cu(1 1 0), the bitartrate molecule is located above the 4-fold hollow site and bonds via both carboxylate groups, with each of the four oxygen atoms located at on-top sites, Fig. 4. A major difference between the Cu(1 1 0) and Ni(1 1 0) systems emerges when the organisation of the bitartrate species is considered. The extended 2D enantiomorphous templates observed in the TA/Cu(1 1 0) system are not created on Ni(1 1 0). Instead, organisation is restricted to 1D chains, and occurs along the main $\langle 1\bar{1}0 \rangle$ symmetry direction, Fig. 5a and b. However, detailed studies by RAIRS, LEED, STM and DFT calculations suggest that the expression of chirality at the surface is, in fact, inducted at an even deeper level [21]. Specifically, adsorption leads to a highly strained bitartrate-Ni$_4$ complex at the surface where a strong asymmetric distortion of the bitartrate skeleton is created alongside a concomitant *reconstruction* of the bonding nickel atoms, which are pulled away from their symmetric positions and twisted to give an oblique unit mesh where all the mirror planes are locally destroyed, Fig. 5d. Thus, the adsorption system possesses arrangements of chiral bitartrate-Ni$_4$ units in 1D lines, where chirality transfer to the surface is mediated by the strong metal–molecule interaction that leads to reorganisation of the underlying metal atoms into chiral arrangements. The general structural conclusions of the DFT calculations are confirmed by detailed analysis of the STM images, Fig. 5c, where the molecular features in the STM images occupy, on average, a space of 6.8 Å × 4.6 Å, in good agreement with the calculated area of 7.04 Å × 4.98 Å [21] containing the relaxed bitartrate-Ni$_4$ complex.

Finally, calculations on polar charge distributions of the bitartrate-Ni$_4$ complex [23] show that the transmission of asymmetry from the adsorbate to the surface is not restricted to a geometrical reorganisation. In fact, the delocalised nature of the molecular wavefunctions leads to direct electronic communication between the molecule's chiral centres and its bonding groups [23]. This leads to the transfer of chirality from the chiral centres to the 4 O–Ni bonds formed, which display an asymmetric character, with one diagonal pair being equivalent and having a bondlength of 2.04 Å, while the opposite diagonal pair possesses a shorter bondlength of 1.94 Å, Fig. 5d. This chiral distribution of bondlength suggests
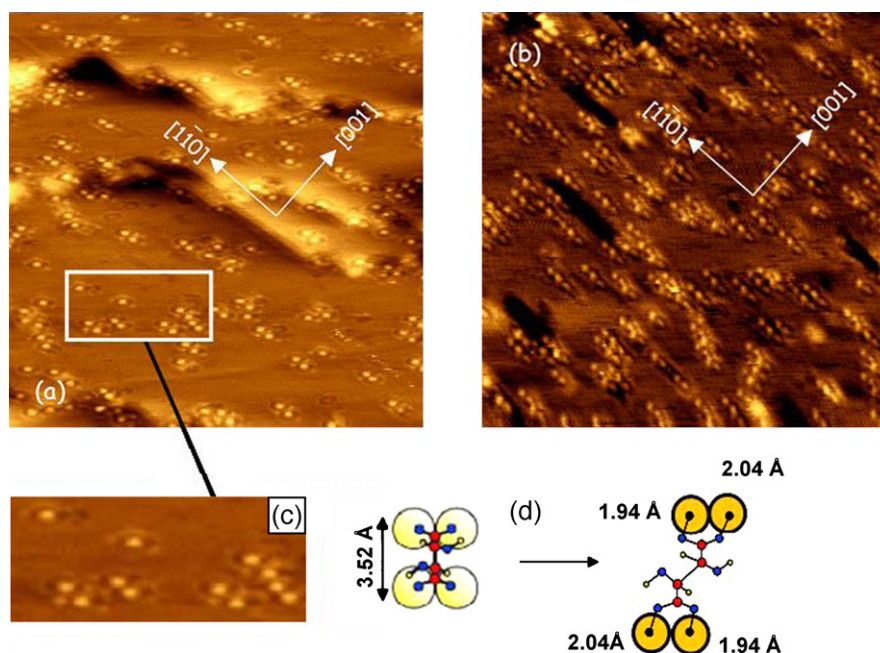

Fig. 5. STM images of (R,R)-tartaric adsorbed on Ni(1 1 0) at room temperature. (a) Low coverage bitartrate species, 300 Å × 300 Å, V = −2.115 V, I(t) = −1.16 nA. (b) Medium coverage bitartrate species, 300 Å × 300 Å, V = −1.76 V, I(t) = −1 nA. (c) Enlarged STM image showing molecular shape and perturbation of the surface, 45 Å × 100 Å, V = −2.115 V, I(t) = −1.16 nA. (d) Schematic showing the adsorption of the bitartrate species on the 4-fold bridge site leading to distortion of both the molecule and the underlying metal atoms. Note the four Cu–O bonds created have a chiral distribution in lengths. Reproduced with permission from Ref. [20], copyright 2004, Elsevier.

that asymmetry may well be communicated into the electronic structure of the adsorption site.

The distortion and underlying reconstruction of the Ni are enantiomer-specific, so that the mirror enantiomer yields the mirror adsorption footprint, with the backbone of the bitartrate molecule distorted in the opposite directions and the underlying metal possessing the mirror chiral reconstruction. This chiral preference is driven by the fact that the energy cost of adopting the 'wrong' mirror distortion is $7\,kJ\,mol^{-1}$ [21]. This energy penalty is enough to ensure that 90% of adsorbates will display a particular handedness and ensure a high degree of asymmetry transmission from the molecule into the metal structure.

6. Conclusions

The understanding of chirality at surfaces via the adsorption of organic molecules has witnessed a real step-change in the past decade and a number of important parameters and phenomena have been revealed by STM, a range of surface spectroscopic techniques and theoretical calculations. The work presented here summarises the salient points of tartaric acid behaviour on Cu(1 1 0) and Ni(1 1 0) surfaces. Although studied under idealised conditions, some fundamental aspects of chiral expression at surfaces have been gleaned, which must manifest themselves in the real catalytic system, albeit in a modified form when solvents and promoters, etc. are present. For example, the myriad of chiral expressions that an organic–inorganic interface can display is an important aspect that must be taken on board as the field tries to move to rational designs for a new generation of heterogeneous enantioselective catalysts. Similarly, the nanoscopic insights built from advanced surface science experiments and high-level density functional theory is beginning to reveal the mechanisms of asymmetric induction and the critical roles of both the organic molecule and the underlying surface in creating the overall chirality. The studies reported here are some of the first detailed mappings of such systems drawn from our laboratory and, no doubt, future studies will create a platform on which to base future design strategies.

References

[1] R.A. Sheldon, Chirotechnology, Dekker, New York, 1993.
[2] V. Dubois, G. Jannes (Eds.), Chiral Reactions in Heterogeneous Catalysis, Plenum, New York, 1995, p. 33.
[3] A. Baiker, H.U. Blaser, in: G.H. Ertl, H. Knoezinger, J. Weinheim (Eds.), Handbook of Heterogeneous Catalysis, vol. 5, VCH, New York, 1997, p. 2442.
[4] C.F. McFadden, P.S. Cremer, A.J. Gellman, Langmuir 12 (1996) 2483.
[5] M. Besson, F. Deblecq, P. Gallezot, S. Neto, C. Pinel, Chem. Eur. J. 6 (2000) 949.
[6] Y. Izumi, Adv. Catal. 32 (1983) 215.
[7] A. Tai, T. Harada, in: Y. Iwasawa (Ed.), Tailored Metal Catalysts, Reidel, Tokyo, 1986, p. 265.
[8] Y. Orito, S. Imai, S. Niwa, J. Chem. Soc. Jpn. (1980) 670.
[9] G. Webb, P.B. Wells, Catal. Today 12 (1992) 319.
[10] H.U. Blaser, H.P. Jalett, M. Muller, M. Studer, Catal. Today 37 (1997) 441.
[11] M. Ortega Lorenzo, S. Haq, P. Murray, R. Raval, C.J. Baddeley, J. Phys. Chem. B 103 (1999) 10661.
[12] M. Ortega Lorenzo, C.J. Baddeley, C. Muryn, R. Raval, Nature 404 (2000) 376.
[13] M. Ortega Lorenzo, V. Humblot, P. Murray, C.J. Baddeley, S. Haq, R. Raval, J. Catal. 205 (2002) 123.
[14] S. Barlow, S. Luoafi, D. Le Roux, J. Williams, C. Muryn, S. Haq, R. Raval, Surf. Sci. 590 (2005) 243.
[15] R. Raval, Curr. Opin. Solid State Mater. Sci. 7 (1) (2003) 67.
[16] S. Barlow, R. Raval, Surf. Sci. Rep. 50 (2003) 201.
[17] S. Barlow, R. Raval, Curr. Opin. Colloid Interface Sci. 13 (2008) 65.
[18] L.A.M.M. Barbosa, P. Sautet, J. Am. Chem. Soc. 123 (2001) 6639.
[19] R. Fasel, J. Wider, C. Quitmann, K.-H. Ernst, T. Greber, Angew. Chem. Int. Ed. 116 (2004) 2913.
[20] C.G.M. Hernse, A.P. Van Bavel, A.P.J. Jansen, L.A.M.M. Barbosa, P. Sautet, R.A. Van Santen, J. Phys. Chem. B 108 (2004) 11035.
[21] V. Humblot, S. Haq, C. Muryn, W.A. Hofer, R. Raval, J. Am. Chem. Soc. 124 (3) (2002) 503.
[22] V. Humblot, S. Haq, C. Muryn, R. Raval, J. Catal. 228 (1) (2004) 130.
[23] W.A. Hofer, V. Humblot, R. Raval, Surf. Sci. 554 (2004) 141.